Multiple Phase Three-dimensional Scenes Encryption Using Computer Generated Holograms

Sherif kishk[a], Tamer H. El-Nagger[a] and Ahmed S.Samra[a]
Electronic and Communication Dept, Faculty of Engineering,
Mansoura University, Egypt.

Summary
In this paper, a method to encrypt and decrypt three-dimensional objects using computer generated holograms and phase encoding is proposed. The amplitude and phase information of a three dimensional object is obtained computationally using phase shifting interferometer and stored on digital computer. Encryption is performed using a random phase mask at a plane located in the Fresnel diffraction region. The decryption key is recorded as a digital hologram. Different images of the three dimensional object at different planes can be restored after the decryption. A comparison between Single and Multiple phases encoding for binary and gray scale images is performed. Bit error rate and mean square error are reported to measure the quality of the decryption process. Results show that multiple phase encoding is more secure than single phase encoding. Also, multiple phase encoding increases the mean square error for the gray scale images.

Keywords:
Optical encryption, Computer-generated-hologram, Phase encoding

1. Introduction

Optical encryption and data security are key issues in optical communication systems for data storage and transmission to protect data from unauthorized access [1-7].Compared to traditional security systems, optical security offers primarily two types of benefits. First, parallel data processing which is more suitable for image encryption and rapid transmission of information [5, 8] .Second, optics provides many degrees of freedom with which the optical beam may be encoded, such as amplitude, phase, wavelength, and polarization[1,9].
Various types of optical information security have been explored [1-12]. Different optical verification systems for information security applications; based on optical correlations has been reported [5]. These systems correlate two functions: first, is the lock, always inside the correlator, and the other, is the key, presented to the system by the user in the verification stage. A material such as light-scattering medium is used to hide image data as an initial stage of data protection, this hiding technique are used to protect data from unauthorized access [8]. Digital holography [12,13] is used for efficient recording of fully complex information with intensity sensors [10,11,15]. Computer generated holography [16,17] is used to record and retrieve the encrypted image of a three dimensional scenes using the principle of digital holography [2,10,11,18-22]. Another method is presented for digital image encryption using computer generated holograms for semi-fragile watermarking with encrypted images [23]. In addition, the technique of fully phase image encryption is a method to encrypt data using double random phase mask, it performs better than amplitude-based encryption in the presence of noise [1-4]. The encryption is performed using two random-phase codes, one placed at the object plane and other is placed at Fresnel [9] or Fourier plane [2-3].
In this paper, a technique for optical encryption of three-dimensional (3D) information using the principle of computer generated holograms (CGH) is presented. The principle of off-axis digital holography [24] is used with single and multiple phases encoding to encrypt the 3D object. A comparison between these techniques is represented and Bit Error Rate (BER) and Mean Square Error (MSE) are reported for Black and White (binary) image and gray scale image, respectively.
In section 2, a discussion of the proposed system is represented. Section 3, presents an analysis for the proposed system. Section 4, introduces the simulation results of single and multiple phase encoding systems. In section 5, performance of the proposed system with brief calculation of BER and MSE for the binary image and gray scale image are discussed. Finally, conclusion is presented in section 6.

2. Proposed System

A security system that combines random phase encryption with a digital holographic technique using computer generated holograms has been proposed. This system enables the encryption of 3D information optically. It is based on Mach-Zehnder [13] interferometer architecture as shown in Figure1.
The proposes interferometer apply the principle of Fresnel diffraction [10,11,26], free-space propagation[24] and

Manuscript received April 5, 2010
Manuscript revised April 20, 2010

CGH[16,17,23]. The Fresnel CGH [14] generated from an object located within a Fresnel region in which the Fresnel diffraction formula is satisfactory valid. For this case, a digital construction of a 3D test scene is performed by slicing the 3D object image into a number of 2D images, each of these images describe the 3D object at different distance from the CCD camera.

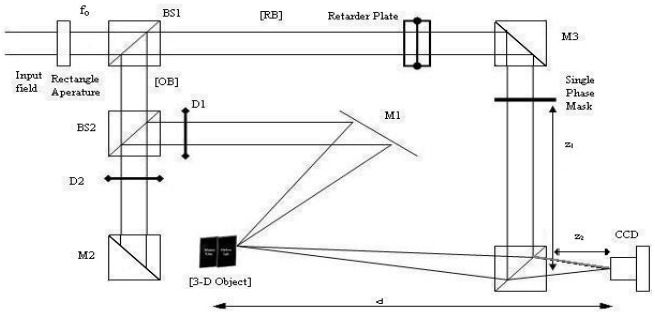

Fg.1.The proposed Mach-Zehnder interferometer

As shown in Figure 1, f_o represents the field emanates from the rectangular aperture propagate into the first beam splitter (BS1). It is splitted into two beams, the first beam is the Object beam (OB) propagates to second beam splitter (BS2), the second beam is the reference beam (RB), propagates to retarder plate. D1 and D2 are diaphragms. M1, M2 and M3 are highly reflected mirrors. BS3 is a beam splitter; and $z=z_1+z_2$ where z is the propagation distance between the random phase mask (RPM) and the CCD plane.

An Argon laser source is used to emit a vertical polarized light beam with λ=541.5nm and has a narrow line width over *(x,y)* plane. It is common to represent this kind of light sources by two dimensional Dirac-delta function, namely, $g(x,y)=\delta(f(x,y))$ where $f(x,y)=0$; defines an arbitrary curve on the *(x,y)* plane, and $\delta(.)$ is the Dirac-delta function [25]. The rectangular aperture modulates the input field dimension by *[L×L]* pixels which determine the final output hologram dimension. The aperture function is represented by $rect\left[\frac{x}{L},\frac{y}{L}\right]$, where *(x,y)* is the input Cartesian coordinates and *L* is an iteger represents the length of aperture. The field f_o is represented by one within the aperture area and zero otherwise. In free space propagation and under Fresnel diffraction approximation [9-11], the field f_o is divided by BS1 into OB and RB by percentage respectively. The OB travel to M1 through the BS2 with D1 open and D2 closed, the OB illuminates the 3D object placed at distance d from a CCD Camera capture the hologram. Two phase retarder plates modulate the RB beam. An interference patterns between OB and RB are recorded with four steps phase shifting $\Delta\varphi_o = 0, \pi/2, \pi, 3\pi/2$. Four interference patterns are stored using the CCD camera. Note that, to reconstruct the 3D object images, the authorized user must have the proper key (or the phase mask), the propagation distance of RPM ($=z_1+z_2$) "distance between phase mask and detector output plane", and the propagation distance d of the 3D object. Assuming that, the input scene, to be encrypted, is consisted of two level binary or gray scale images as shown in Figure 2, and Figure 3, respectively. These two images are located at different distances d_1 = 0.25m, and d_2 = 0.26m from the detector output plane. For binary image, the pixel value between 0 and 1, while the pixel value for gray scale image ranges between 0 and 255.

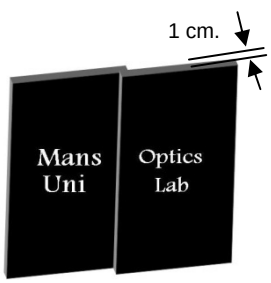

Fig.2. Binary 3D object to be encrypted

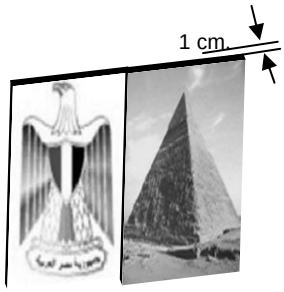

Fig.3. Gray Scale 3-D object to be encrypted.

Two different optical encryption methods are performed with two different types of objects "binary" object and "gray scale" object, in the first encryption method "single phase encoding", only one random phase mask (RPM) is used as an encryption key and placed at distance $z=z_1+z_2=0.1$m from the detector output plane. This RPM has random distribution phase function $f(x,y)=\exp[j2\pi R(x,y)]$ where *(x,y)* are the spatial dimension and *R(x,y)* is a uniformly distributed random variables from 0 to 1. In the second encryption method ,Multiple phase encoding, *N* random phase encoding masks are used. These *N*-RPM are placed at different distances from the output plane; this will add degrees of freedom to the encryption system. These factors are the phase mask function of each RPM, its 3D location from the hologram plane and the order of these *N*-RPM.

Figure 4 shows a diagram for the encryption and decryption processes. The encryption processes is performed by applying a plane wavefront that illuminates an input object and reference phase mask, the interference pattern of these two waves produces the amplitude A_E and phase φ_E of the encrypted image as shown in Fig.4 (a)[9]. The decryption key amplitude A_k and phase key φ_k are obtained by illuminating the reference phase mask with the last plane wave front as shown in Fig.4 (b)[9]. The decryption process is performed by using the amplitude and phase of the encrypted image and decrypting key, the input object image can be reconstructed by applying inverse Fresnel-Kirchhoff integral with the proper distance as shown in Figure 4(c)[9].

3. Analysis

Assuming that, the 3D input object is an opaque scene illuminated by OB that is a Dirac-delta field function emanate from a point source. In this way, the complex amplitude distribution at the output plane $U_o(x,y)$ [26] is evaluated with the following 3D integrals of superposition;

$$U_o(x,y) = A_o(x,y)\exp[i\varphi_o(x,y)] = \frac{1}{i\lambda}\iiint_{-\infty} O_o(x',y';z)\times\frac{1}{z}\exp\left[i\frac{2\pi}{\lambda}z\right]\times\exp\left[\frac{\pi}{\lambda z}\left[(x-x')^2+(y-y')^2\right]\right]dx'dy'dz \quad (1)$$

Where z is the RPM propagation distance, λ; is the wavelength of the incident light and $A_o(x,y)$ and $\varphi_o(x,y)$ are the amplitude and phase of the complex amplitude distribution at the output plane generated by the object beam. $O_o(x',y';z)$ describes the light reflected from the opaque 3D object.

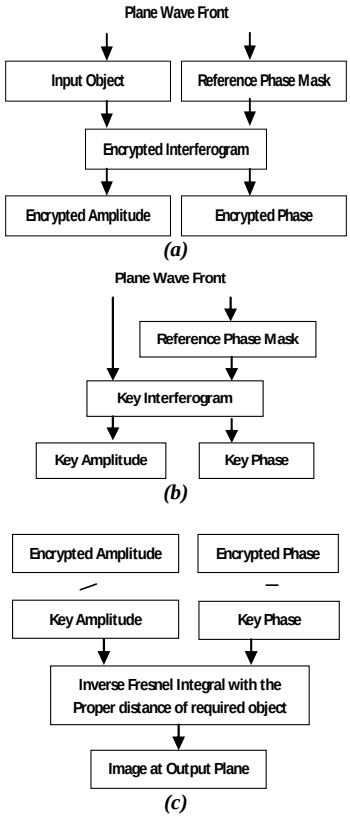

Fig.4. Diagram of the Encryption-Decryption process. (*a*) Encryption, (*b*) Decrypting Key, (*c*) Decryption.

The RB propagates through two retarder plates to the mirror M3. This retarder plates modulate the wave by phase function $\Delta\varphi$. Then this wave propagates through a random phase mask and BS3 to the output plane. A random phase mask is a plate that has a uniform random phase distribution [0 to 2π] over its dimension [256×256] pixels, and used as a key of encryption. The two retarder plates are half-wave plate and quarter-wave plate. These plates modulate the phase of the RB with phase shift $\Delta\varphi_p = 0, \pi/2, \pi, 3\pi/2$ [10,11,24,25] by suitable orientation of fast and slow axes of the retarder plates with the polarization of the incident light. For each one of the four phase shifts, an interferogram is recorded. According to the generated complex field [19] for each phase shift $\Delta\varphi_p$ and under Fresnel diffraction integrals;

$$U_R(x,y;\Delta\varphi_p) = A_R(x,y)\exp[i(\varphi_R(x,y)+\Delta\varphi_p)] = \exp[i\Delta\varphi_p]\exp\left[i\frac{\pi}{\lambda l}(x^2+y^2)\right]\cdot\int\int_{-\infty}^{\infty}\exp[i\varphi(x',y')]\exp\left[-i\frac{2\pi}{\lambda l}(xx'+yy')\right]dx'dy' \quad (2)$$

Where A_R, and φ_R represents the RB amplitude and phase at the original plane, when both fast axes of the retarder plates are aligned with the direction of polarization. i.e. when the phase shift interferometer, $\Delta\varphi_p=0$. At the output plane, the recorded intensity pattern is given by [24]:

$$I_p(x,y;\Delta\varphi_p) = \left|U_o(x,y)+U_R(x,y;\Delta\varphi_p)^2\right| \quad (3)$$

Where U_o and U_R given by Equation (1) and (2), respectively. Since a random phase function is used with the RB, the intensity pattern at the output plane will be a random intensity distribution. Denoting the complex amplitude distribution of the OB and RB at the output plane with $U_o(x,y) = A_o(x,y)\exp[i\varphi_o(x,y)]$ and $U_R(x,y;\Delta\varphi_p) = A_R(x,y)\exp[i(\varphi_R(x,y)+\Delta\varphi_p)]$, respectively, Equation (3) can be written as;

$$I_p(x,y;\Delta\varphi_p) = [A_o(x,y)]^2+[A_R(x,y)]+2A_o(x,y)A_R(x,y)\cos(\varphi_o(x,y)-\varphi_R(x,y)-\Delta\varphi_p) \quad (4)$$

Using the previous values of $\Delta\varphi_p$, four interference patterns are computed numerically by applying CGH principle. Also, the encrypted phase and amplitude of the recorded hologram obtained by;

$$\varphi_E(x,y) = \varphi_o(x,y)-\varphi_R(x,y) = \tan^{-1}\left[\frac{I(x,y;-3\pi/2)-I(x,y;-\pi/2)}{I(x,y;0)-I(x,y;-\pi)}\right] \quad (5)$$

$$A_E(x,y) = \frac{1}{4}\frac{I(x,y;0)-I(x,y;-\pi)}{\cos(\varphi_o(x,y)-\varphi_R(x,y))} \quad (6)$$

$$I_E(x,y)=A_E(x,y)\exp[i\varphi_E(x,y)] \quad (7)$$

where $I_E(x,y)$, $A_E(x,y)$ and, $\varphi_E(x,y)$ are the encrypted complex output hologram, amplitude of the output hologram and its phase, respectively. The output hologram is encrypted using the random phase key and its position. The decryption hologram is recorded when the diaphragm D2 is opened, D1 is closed, and the object is removed from the propagation path. In this case, four-hologram are recorded and the decryption key function is given by;

$$\varphi_k(x,y) = \varphi_c(x,y) - \varphi_R(x,y) = \tan^{-1}\left[\frac{I'(x,y;-3\pi/2) - I'(x,y;-\pi/2)}{I'(x,y;0) - I'(x,y;-\pi)}\right] \quad (8)$$

$$A_k(x,y) = \frac{1}{4}\frac{I'(x,y;0) - I'(x,y;-\pi)}{\cos(\varphi_c(x,y) - \varphi_R(x,y))} \quad (9)$$

$$, I_k(x,y) = A_k(x,y)\exp[i\varphi_k(x,y)] \quad (10)$$

Where A_c and φ_c are the constant amplitude and phase of the object beam, respectively, they can be substituted by 1 and 0 [10 Also, I_k is the encrypted complex key, A_k and φ_k are its amplitude and phase, respectively. Now, using the decrypting key, the decrypted image of 3D scene can be obtained using the following equations [10],

$$\varphi_D(x,y) = \varphi_E(x,y) - \varphi_k(x,y) \quad (11)$$

$$A_D(x,y) = \begin{cases} \frac{A_E(x,y)}{A_k(x,y)} & A_k(x,y) \neq 0 \\ 0 & otherwise \end{cases} \quad (12)$$

$$I_D(x,y) = A_D(x,y)\exp[i\varphi_D(x,y)] \quad (13)$$

Where A_D and φ_D are the amplitude and phase of the decrypted Fresnel hologram. $U_D(x,y)$, is the required detected image of 3D object. Now, using free space propagation, the amplitude distribution of the input object can be reconstructed.

4. Simulation Results

A simulation for the proposed encryption system by applying Fresnel diffraction approximation is conducted. Free space propagation principles are applied to simulate the propagation of plane wave field through object and reference path to the hologram output plane.

For the binary 3D scene of Figure 2, the amplitude and the phase of the encrypted output hologram using single phase mask are shown in Fig. 5(a) and Fig. 5(b), respectively. The decryption key amplitude and phase obtained from equations (8, 9) are shown in Fig 6(a) and Fig 6(b), respectively.

For the 3D gray scale object of figure 3, the amplitude and the phase of the encrypted output hologram are obtained from equations (5, 6) as shown in figure 8(a) and figure 8(b), respectively. Figure 9(a) and figure. 9(b), show the reconstructed 3D scene at d_1 = 0.25m, and d_2 = 0.26m respectively.

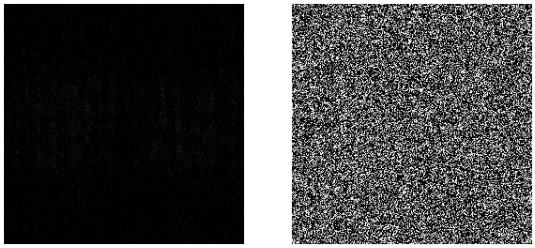

(a) *(b)*

Fig.5, Encrypted Hologram of binary 3D scene. *(a)* **Amplitude,** *(b)* **Phase.**

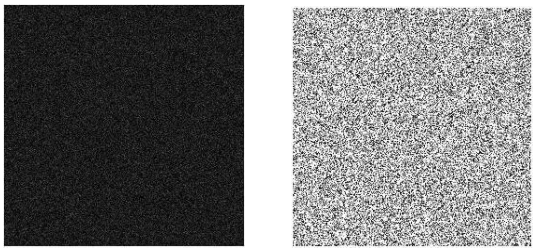

(a) *(b)*

Figure 6, key Hologram. (*a*) Amplitude, (*b*) Phase.

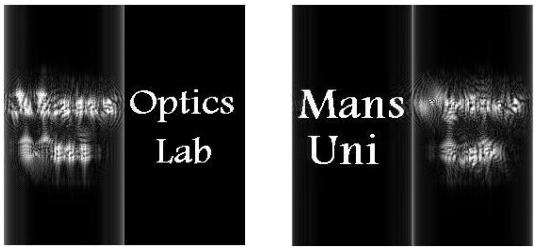

(a) *(b)*

Fig.7, Reconstructed 3D binary scene using single phase mask. *a*) at d_1=0.25m, (*b*) at d_2=0.26m.

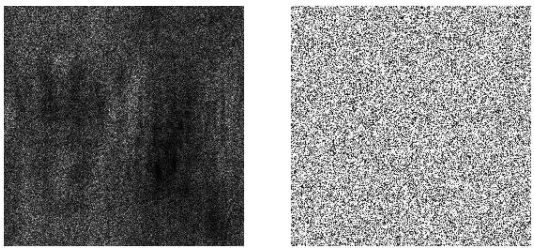

(a) *(b)*

Fig.8. The encrypted output hologram for gray scale scene. (*a*) Amplitude. (*b*) Phase.

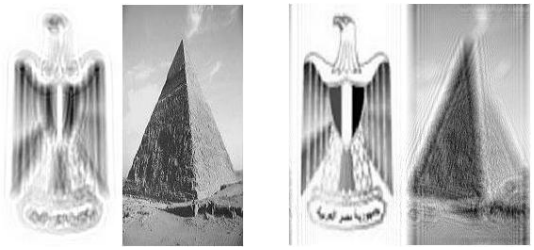

(a) *(b)*

Fig.9 The retrieved 3D gray scale scene using single phase mask.. (*a*) at distance d1= 0.25m, (*b*) at distance d2= 0.26m.

Applying equations (11, 12), and substitute in equation (13), the decrypted 3D scene, constructed at distance d1 = 0.25m, and d2 = 0.26m, respectively, are shown in Fig. 7(a) and Fig. 7(b).

Now, the system is tested using multiple phase masks instead of single one, where more than one phase mask are placed in the reference beam path. In this method 5 RPM's are used to encrypt the transmitted image. These phases are placed in the RB propagation distance at z = 0.1m, 0.11m, 0.12m,0.13m, and 0.14m respectively. For the 3D binary scene shown in Figure 3, the amplitude and the phase of the encrypted output hologram are obtained from equations (5) and (6) as shown in Fig. 10(a) and Fig. 10(b), respectively. Fig. 11(a) and Fig. 11(b), show the amplitude and phase of the decryption key hologram, respectively. Fig. 12 shows the reconstructed 3D binary scene using the correct RPMs placed at the correct order and correct places at a distance d_1 = 0.25m, and d_2 = 0.26m, respectively.

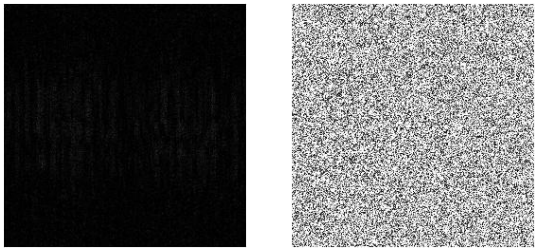

(a) *(b)*

Fig.10. the encrypted Hologram for a 3D binary scene using multiple RPM (*a*) Amplitude, (*b*) Phase.

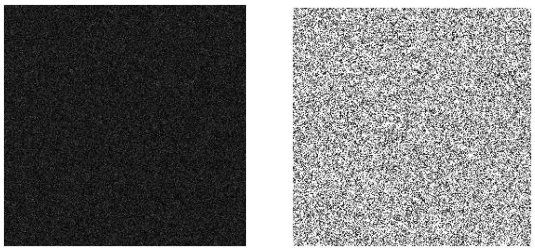

(a) *(b)*

Fig.11. Multiple phase key hologram. (*a*) Amplitude, (*b*) Phase

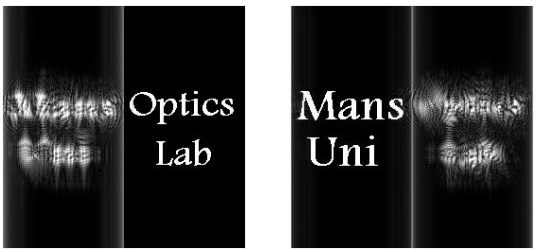

(a) *(b)*

Fig.12. The reconstructed 3D binary scene using the correct 5 phase masks. (*a*) at d_1=0.25m, (*b*) at d_1=0.26m

The multiple phase masks encoding system is tested now for 3D the gray scale scene shown in Figure 3. Figure 13 shows the reconstructed gray scale 3D scene using the correct RPM placed at the correct order and correct places for different reconstruction distances. As seen at d=0.25m the right part of the scene appears distorted, and at d=0.26m the left part appears distorted.

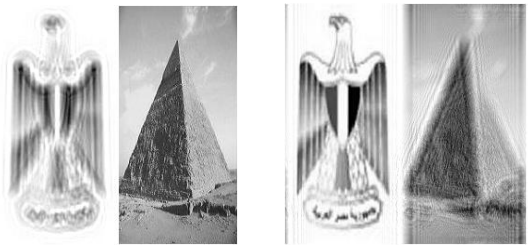

(a) *(b)*

Fig.13 the retrieved 3D gray scale scene using 5 phase masks. (a) at a distance d_1= 0.25m, (b) at a distance d_2= 0.26m

The simulations show that, only the scene part at the correct reconstruction distance is clearly retrieved. Also, the proposed encryption system has three encryption keys. These keys are the propagation distance between the object and the CCD output plane, phase mask function and the order of the phases in case of multiple phase mask.

5. System Performance

In this section, the system performance for both single and multiple phase encoding is tested against the system encryption keys. These keys are the propagation distance between the 3D object and CCD output hologram, the phase function of the RPM and the order of the RPM's in case multiple phase encoding. The impact of these keys on Bit-Error-Rate [8] (BER) and Mean-Square-Error [4] (MSE) are reported depending on the type of images. Where BER, is the percentage of number of pixels with errors divided by the total number of pixels, and MSE is calculated between the original image and the retrieved image using equation (14) relative to the image intensity.

$$MSE = \frac{\sum_{y=1}^{Y}\sum_{x=1}^{X}\left[O(x.y) - |R(x,y)|\right]^2}{\sum_{y=1}^{Y}\sum_{x=1}^{X}\left[O(x.y)\right]^2}$$

Where *X, Y* are the object dimensions, *O(x,y)* is the original image, and *R(x,y)* is the retrieved image.

First, the effect of the propagation distance and RPM function on the BER for binary scenes is tested when using both single and multiple phases mask encoding. Figure 14 shows the effect of propagation distance d between the 3D object and CCD output plane on the BER for single and multiple phase encoding. This figure shows that there are two minimum BER points at the exact location of the image paths. Also, the performance of both single phase and multiple phase encryption methods is almost identical. Figure 15 and Figure 16 show the effect of propagation distance z between the RPM and CCD output plane on the BER for single and multiple phases encoding, respectively. These figures are created individually for the 3D scene parts at d_1 = 0.25m, d_2 = 0.26m and RPM propagation distance z = 0.1m. Figure 16 shows the effect of the first RPM propagation distance only where the propagation distances for the rest RPMs are correct. These figures show that there is a minimum BER point at the exact location of the RPM.

Figures 15 and 16 show that multiple phase encryption has a slightly higher sensitivity to the phase mask location. The next experiment explores the effect of the phase mask key on the decrypted scene. Figure 17(a) shows the retrieved 3D binary scene at the exact location of the image path at d_1 = 0.25m when single phase encoding is used with wrong phase mask. These images are indistinguishable and the decoder failed to recover the 3D scene. Figure 17(b) shows the effect of change the function of the first RPM at z = 0.1m when multiple phase encoding is used. Figure 17(c) decrypt the 3D scene at a distance of 0.25m for multiple phase encoding when the first RPM is replaced with the fifth RPM. Also, the effect of the propagation distance and RPM function on MSE for gray scale scenes is tested when using both single and multiple phase mask encoding.

Fig. 18 shows the effect of propagation distance d between the 3D gray scale scene and CCD output plane on the MSE for single and multiple phase encoding. This figure shows that there are two minimum MSE points at the exact location of the scene planes. Also, the performance of both encryption methods is similar. Fig. 19, and Fig. 20, show the effect of propagation distance z between the RPM and CCD output plane on the MSE for single and multiple phases encoding respectively. These figures are created for the 3D object scene at the correct distances and RPM propagation distance z = 0.1m. Fig 20, shows the effect of the first RPM propagation distance only where the propagation distance z for the rest RPMs are keept correct.

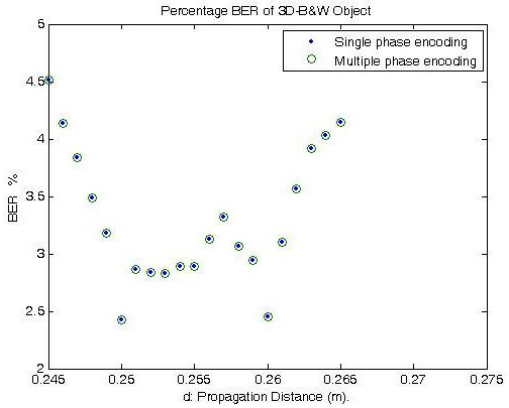

Fig.14. BER for Single and Multiple Phase encoding for different propagation distances for the binary 3D scene

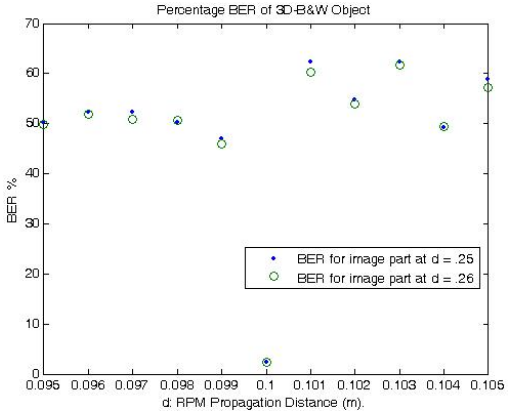

Fig.15 The BER for Single Phase encoding for different phase mask distance for the 3D binary scene

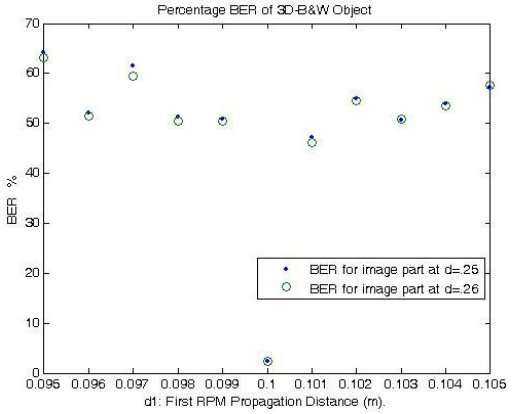

Fig.16, BER for Multiple Phases encoding of Object against first phase distance

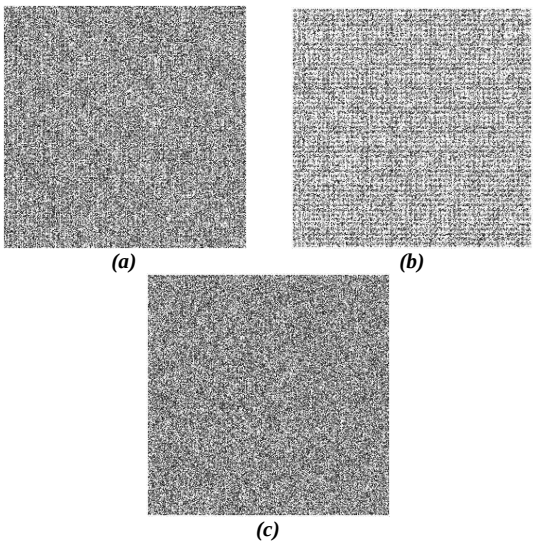

Fig.17. The reconstructed 3D scene when using incorrect phase mask (a) incorrect single phase mask (b) Incorrect first RPM out of 5 RPMs (c) Incorrect RPM order when using 5 RPMs

From the previous discussion, the specified encryption system depends on three encryption keys. These keys are the propagation distance, the RPM function (phase distribution) and the order of the RPM's when multiple phase encoding used. Any encryption system can't be fully dependent on the propagation distance between the object and hologram output plane only where, any unauthorized user can scan for the real image distance. SOm the proposed multiple phase mask optical encryption system provides a robust 3D scene encryption systyem as an change in the RPM or its order distroies the reconstructed 3D scene. The encryption system is fully dependent on the RPM propagation distance, phase function and the order of the multiple masks. Multiple phase encoding performs very efficient but it has a slightly lower MSE compared to single phase encoding when gray scale images are used.

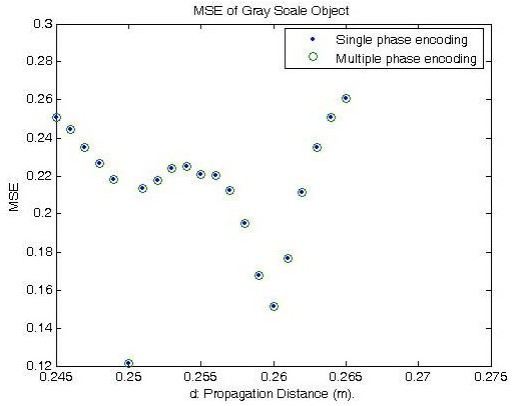

Fig.18 MSE for Single and Multiple Phase encoding for different scene propagation distances

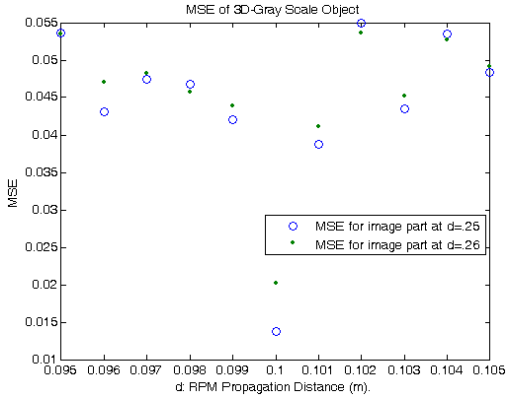

Fig.19 MSE for a 3D gray scale scene using single phase mask against RPM propagation

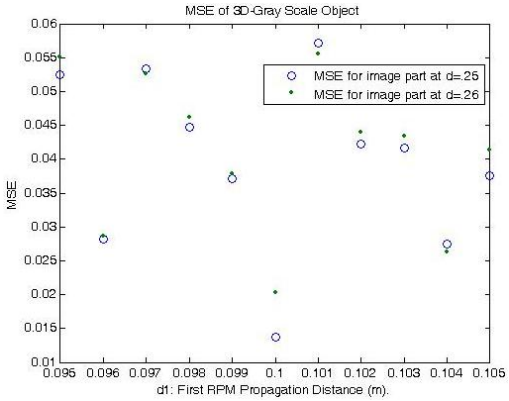

Fig.20. MSE for a 3D gray scale scene using multiple phase masks against the first RPM propagation distance

6. Conclusion

In this paper a CGH method is used to encrypt a 3D scene using random phase mask. Single and Multiple phase masks are used. The proposed multiple-Phase encoding is more secure than Single-Phase encoding but it adds a noise in the case of 3D gray-scale scenes compared to Black & White scenes. The performed simulations showd that the system is very sensitive to the encryption parameters which are the RPM function, and the order of RPM in case of multiple phase encoding and weekly dependent on the object propagation distance where user can scan for right object distance.

References

[1] X. Tan, O. Matoba, T. Shimma, K. Kuroda, and B. Javidi, "Secure optical storage that uses fully phase encryption, "Appl. Opt. vol.39, No.(35), pp.6689-6694, 2000.

[2] B. Javidi, and T. Nomura, "Securing information by use of digital holography," Opt. Lett.vol.25, No.1, pp.28-30, 2000.

[3] P. Refregier and B. Javidi, "Optical image encryption based on input plane and Fourier plane random encoding," Opt. Lett.vol.20, No.7, pp.767-769, 1995.

[4] E. Rueda, J. F. Barrera, R. Henao, R. Torrob, " Optical encryption with a reference wave in a joint transform correlator architecture," Optics Communications, vol.282, No.16, pp.3243- 3249, 2009.
[5] Y. Li, K. Kreske, and J. Rosen, "Security and encryption optical systems based on a correlator with significant output images," Appl. Opt. vol.39, No.29, pp.5295-5301, 2000.
[6] C. H. Yen, H. Chang, H. C. Chien, and C. J. Kuo, "Design of cascaded phase keys for a hierarchical security system," Appl. Opt. vol.41, No. 29, pp.6128-6134, 2002.
[7] N. Singh, A. Sinha. "Optical image encryption using Hartley transform and logistic map", Optics Communications, Vol. 282, vol.282, No. 6, pp. 1104-1109, 2009.
[8] Y. Hayasaki, Y. Mastuba and A.Nagaoka, H. Yamamoto, N. Nishida, "Hiding an image with a light-scattering medium and use of a contrast-discrimination method for readout" Appl. Opt. vol.43,No. 7, pp.1552-1558, 2004.
[9] E. Tajahuerce, O. Matoba, S. C. Verrall and B. Javidi, "Optoelectronic information encryption with phase-shifting interferometer," Appl. Opt. 39(14), 2313- 2320(2000).
[10] E. Tajahuerce, and B. Javidi, "Encrypting three-dimensional information with digital holography," Appl. Opt. vol.39, No.35, pp. 6595- 6601, 2000.
[11] T. J. Naughton and B. Javidi, "Compression of encrypted three-dimensional objects using digital holography" Opt. Eng. Vol.43, No.10, pp.2233-2238,October 2004.
[12] R. El Sawda, A. Alfalou and H. Hamam,"Color Video Sequences Encryption/Decryption Processes Using Several Color Keys Images" International Journal of Security and its applications,Vol. 2, No. 2, April, 2008.
[13] U. Gopinathan, D. S. Monaghan, B. Hennelly, C. P. Mc Elhinney, D. P. Kelly, J. B. McDonald, T. J. Naughton, and J. T. Sheridan," A Projection System for Real World Three-Dimensional Objects Using Spatial Light Modulators", Journal of Display Technology, Vol.4, No.2, June 2008.
[14] CAO Yu-ru, WEI Sui, "Fractional Fourier digital holography," Journal of Communication and Computer, Vol. 4, No.5 (Serial No.30), pp.52-56, May 2007.
[15] E. Shortt, T. J. Naughton and B. Javidi, "Histogram Approaches for Lossy Compression of Digital Holograms of Three-Dimensional Objects," IEEE Trans. Image. Proc. Vol.. 16, No.6, pp.1548-1556, 2007.
[16] D. Abookasis and J. Rosen, "Three types of computer-generated hologram synthesized from multiple angular viewpoints of a three-dimensional scene," Appl. Opt. vol.45, No. 25, pp.6533-6538, 2006.
[17] C. Lopez and J. C. Gutierrez, "The generation of nondiffracting beams using inexpensive Computer Generated Holograms," Am. J. Phys. Vol.75, No. 1, pp. 36-42, January 2007.
[18] J. Gass, A. Dakoff, and K. Kim, "Phase imaging without 2π ambiguity by multiwavelength digital holography" Opt. Lett. Vol.28, No.13, pp.1141-1143, 2003.
[19] J. G. Sucerquia, J. H. Ramirez, and R. Castaneda. "Incoherent Improvement Of the Spatial Resolution in digital holography". United Nations Educational Scientific and Cultural Organization and International Atomic Energy Agency, 1-8, October 2005.
[20] A. Dakoff, J. Gass, and M. K. Kim. "Microscopic three-dimensional imaging by digital interference holography" Journal of Electronic Imaging, pp.643-647, October 2003.
[21] "DHM (Digital Holography Microscope) for imaging cells".
[22] E. Cuche, P. Marquet, and C. Depeursinge. "Spatial filtering for zero-order and twin-image elimination in digital off-axis holography" Appl. Opt. vol.39, No. 23, pp.4070-4075, 2000.
[23] G. S. Spagnolo and M. D. Santis, "Computer Generated Hologram for SemiFragile Watermarking with Encrypted Images," International Journal of Signal Processing, vol. 4, No. 2, pp.133-141, 2007.
[24] M. Hami, A. Kiasatpour, and M. Soltanolkotabi, "Wave Front Reconstruction from Off-Axis Holograms Using Four-Quarter Phase Shifting Method," Journal of Sciences, Islamic Republic of Iran vol.18, No. 1, pp.67-74, 2007.
[25] M. G. Sicairos and J. C. G. Vega, "Two-dimensional Fourier transform of scaled Dirac delta curves" J. Opt. Soc. Vol.21. No.9, pp.1682-1688, sept. 2004.
[26] J. W. Goodman, "Introduction to Fourier optics," (McGraw-Hill, New York, 1968).